Global Excitation of Magnetospheric Plasma Waves: Role in Radiation Belt Dynamics

1. Review of properties of plasma waves in the magnetosphere.
2. Modeling global wave excitation processes.
3. Modeling pitch-angle and energy diffusion rates
4. Multi-dimensional scattering codes.
5. Possible importance of non-linear processes.

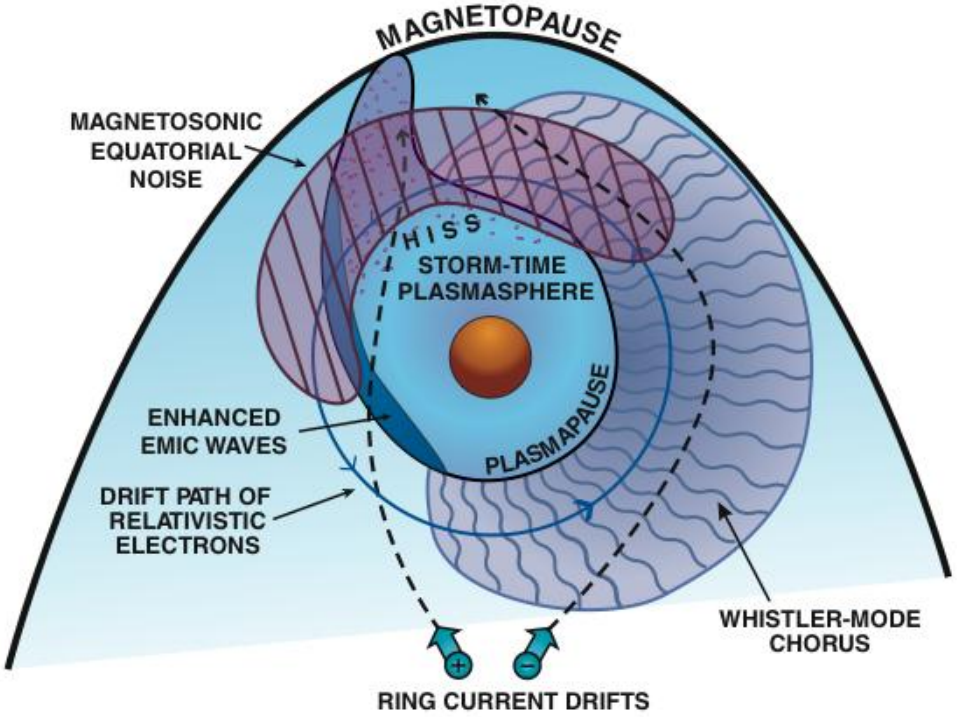

Richard M. Thorne, Jacob Bortnik, Wen Li, Xin Tao, and Lunjin Chen, UCLA

RBSP Science Working Group, Boulder CO, August 2010

Waves in the Magnetosphere Which Affect Electron Dynamics

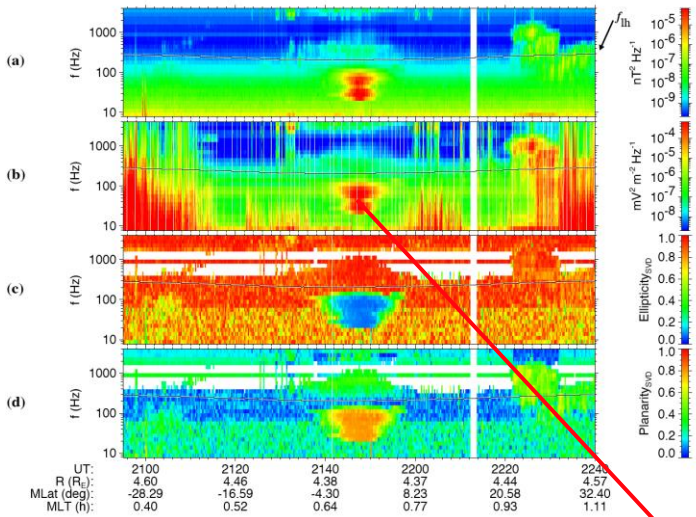

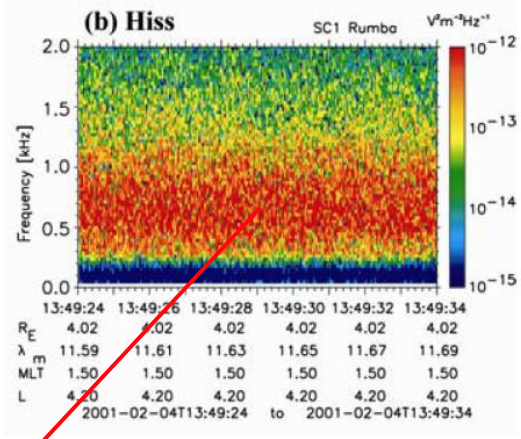

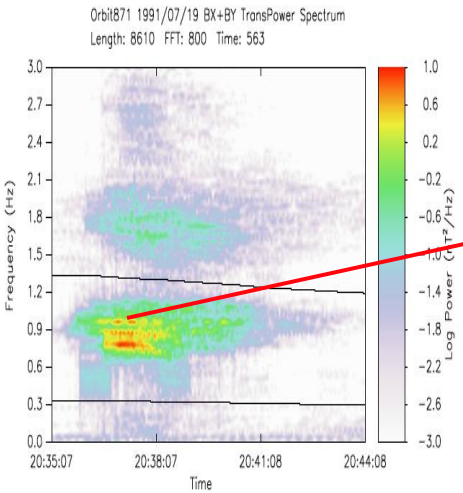

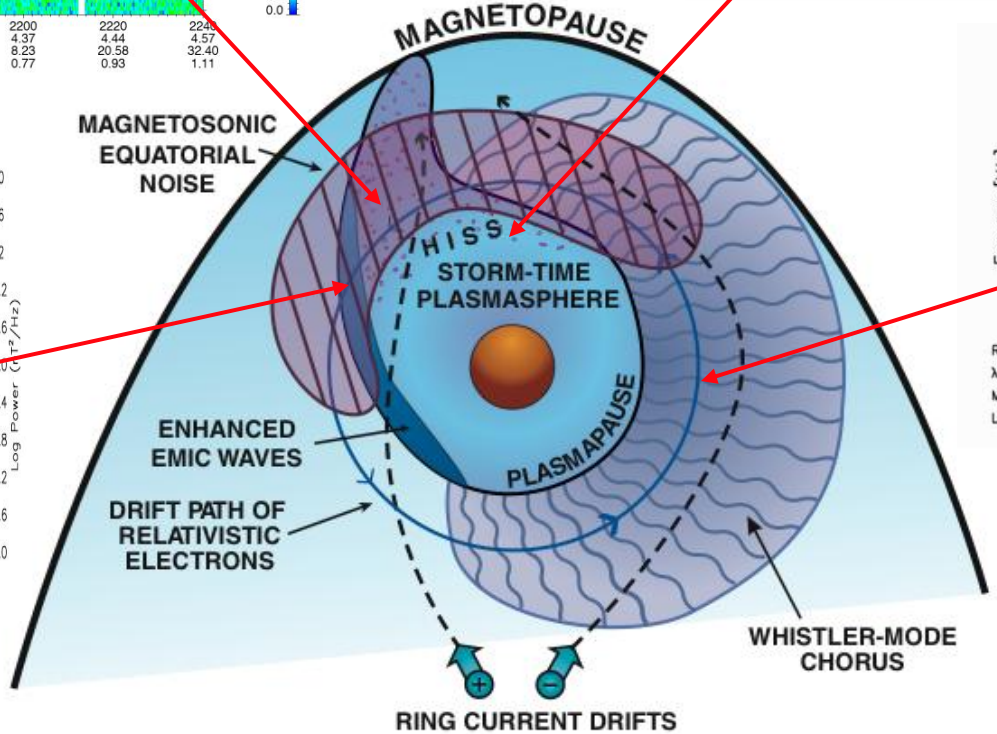

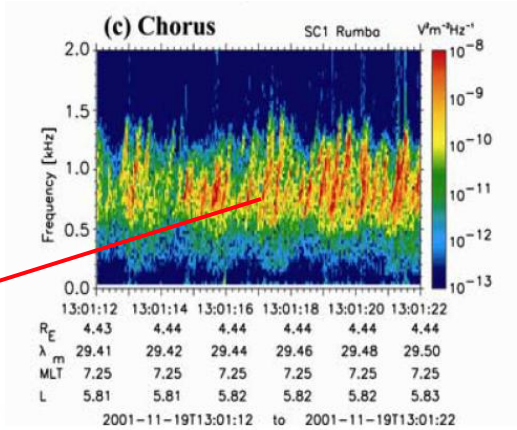

Chorus Excitation Event Observed on CRRES

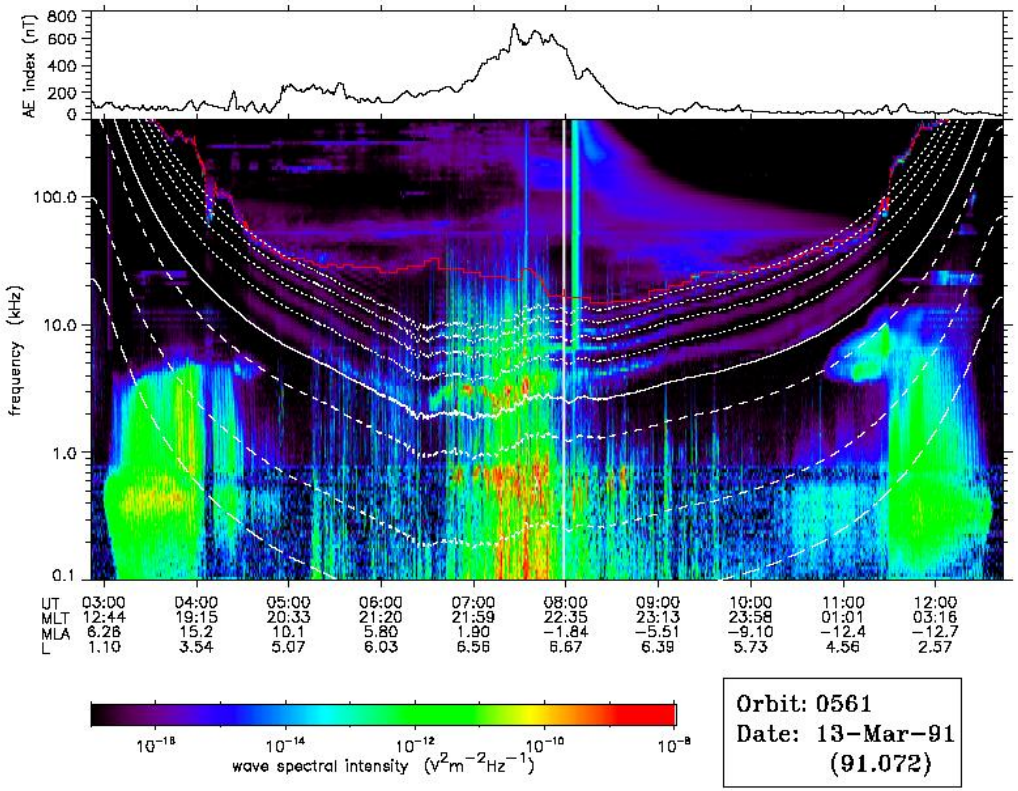

Li et al., JGR, 2008

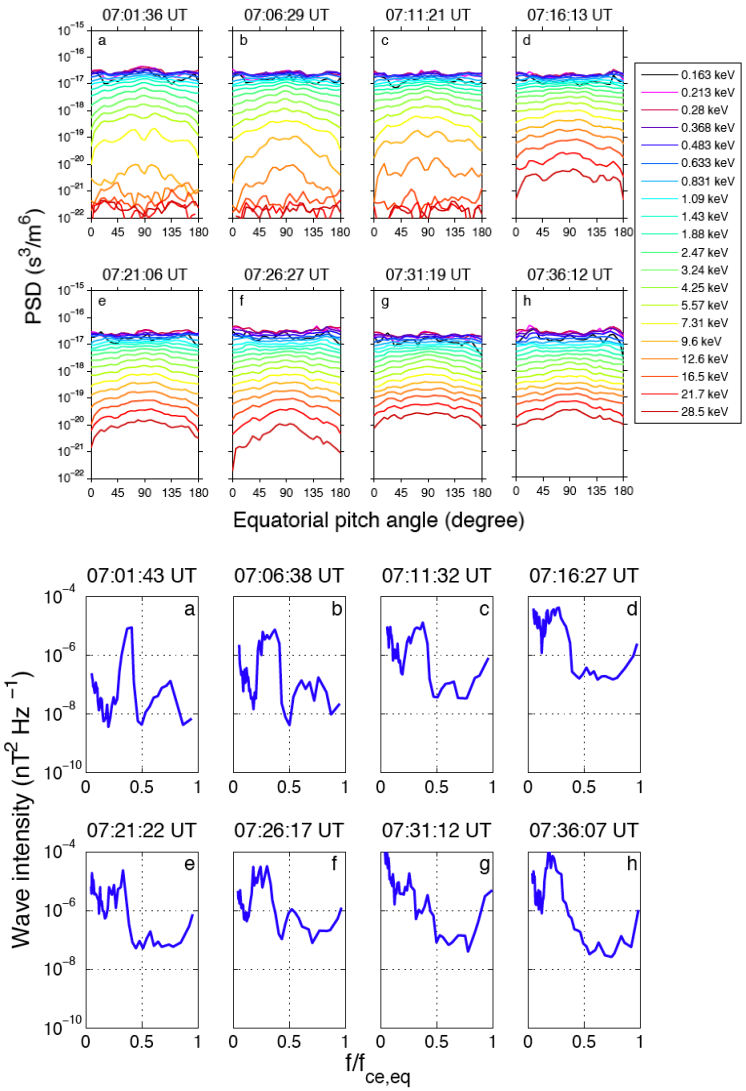

Chorus is excited during the injection of low-energy anisotropic plasma sheet electrons into the inner magnetosphere during enhanced convection. Path integrated gain can be > 100 db and oblique waves are ultimately subject to Landau damping.

Cyclotron Resonant Electron Energies: Li et al., 2009

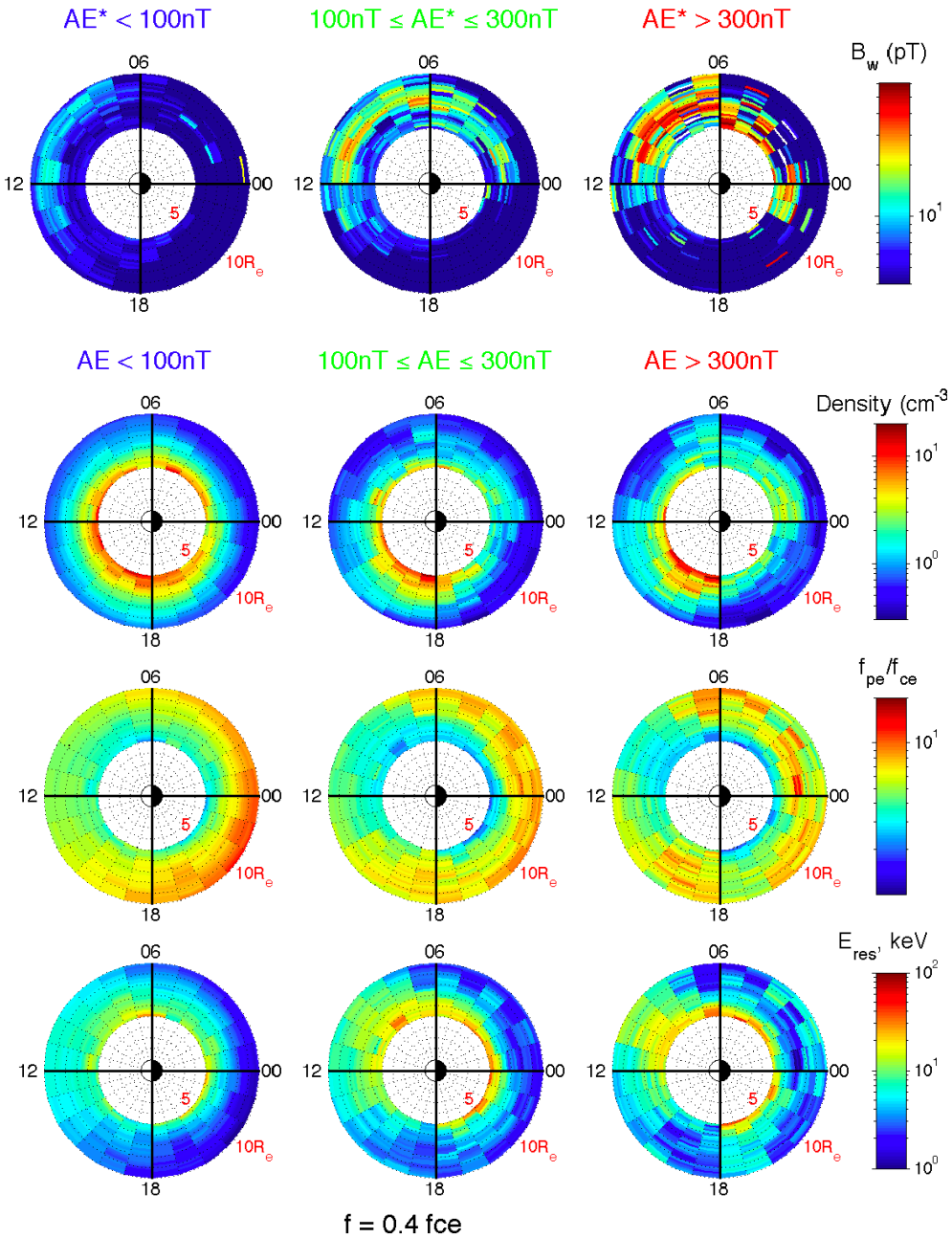

$$E_{res} = (f_{ce}/f_{pe})^2 \, (mc^2/2) \, (f_{ce}/f)(1-f/f_{ce})^3$$

Density obtained from THEMIS SC potential.

Magnetic field from onboard magnetometer.

Lower band chorus with $f=0.4\ f_{ce}$ resonates with ~5 keV electrons on the nightside and 20 keV electrons on the dayside.

Occurrence rate of chorus waves for different wave amplitudes

Li et al., GRL 2009

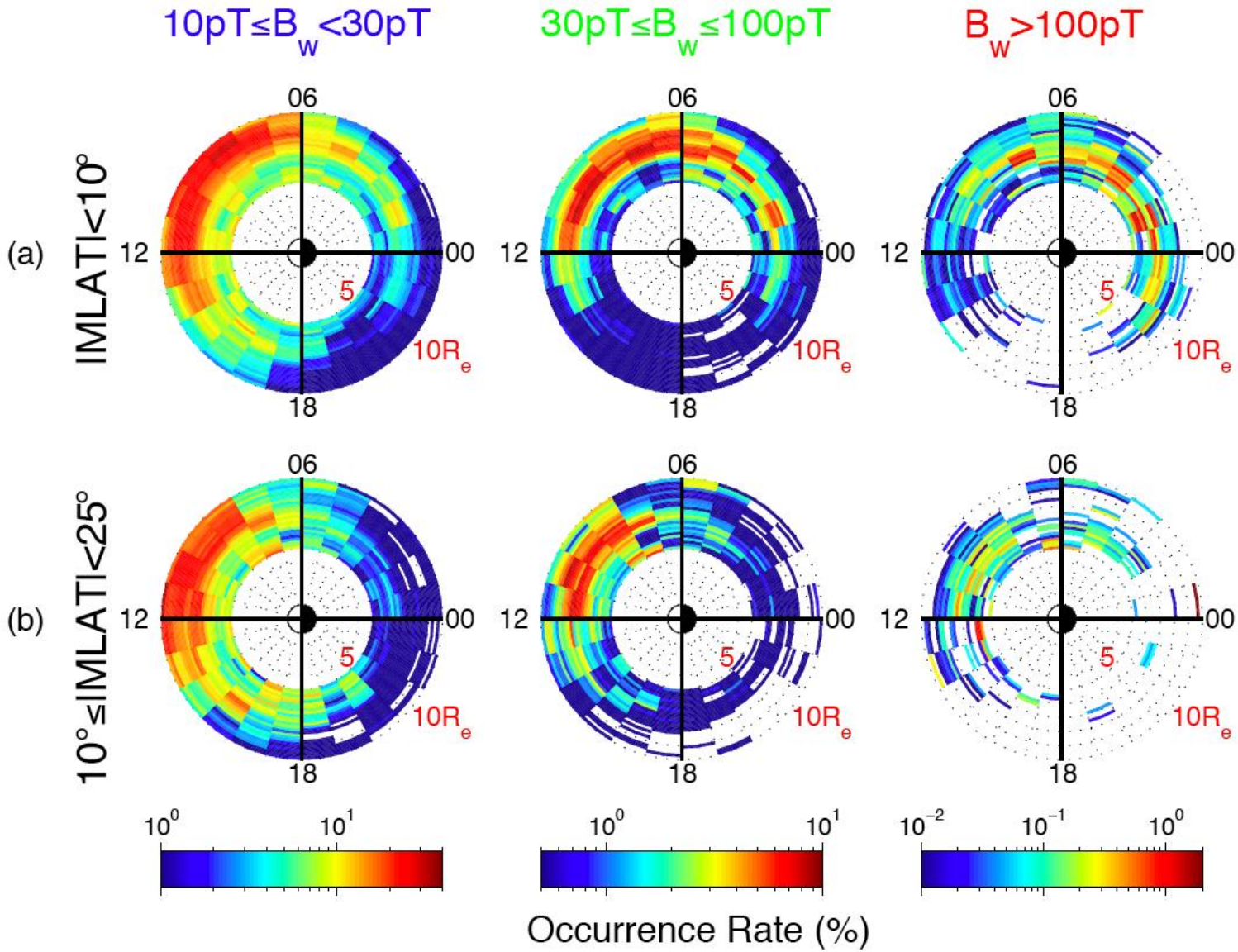

Non-linear Scattering by Large Amplitude Chorus

Bortnik et al. GRL, 2008

Chorus is a discrete coherent emission, probably non-linear.

Extremely large amplitude chorus B_w> nT are occasionally observed.

Role of non-linear scattering, phase bunching and trapping in large amplitude waves B_w> nT

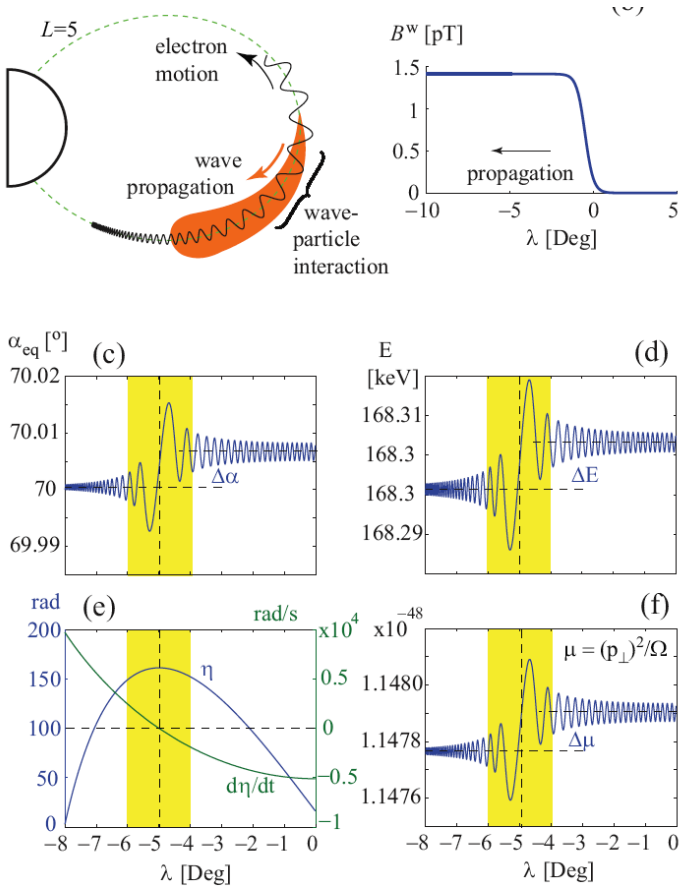

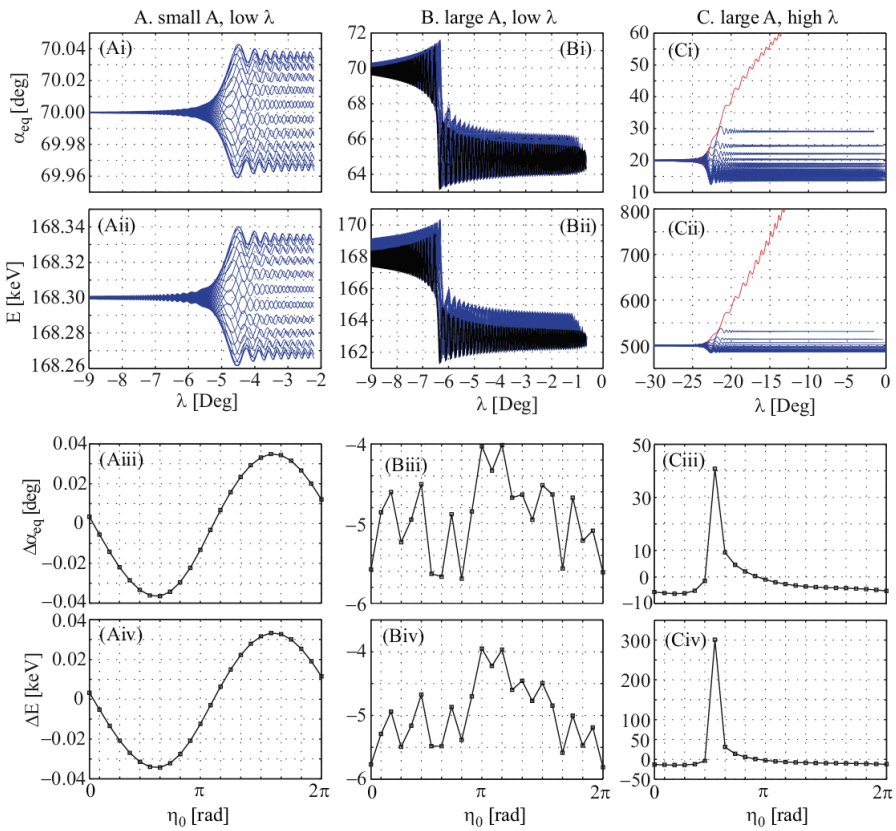

RAM Simulation of Electron Injection

Jordanova et al., 2010

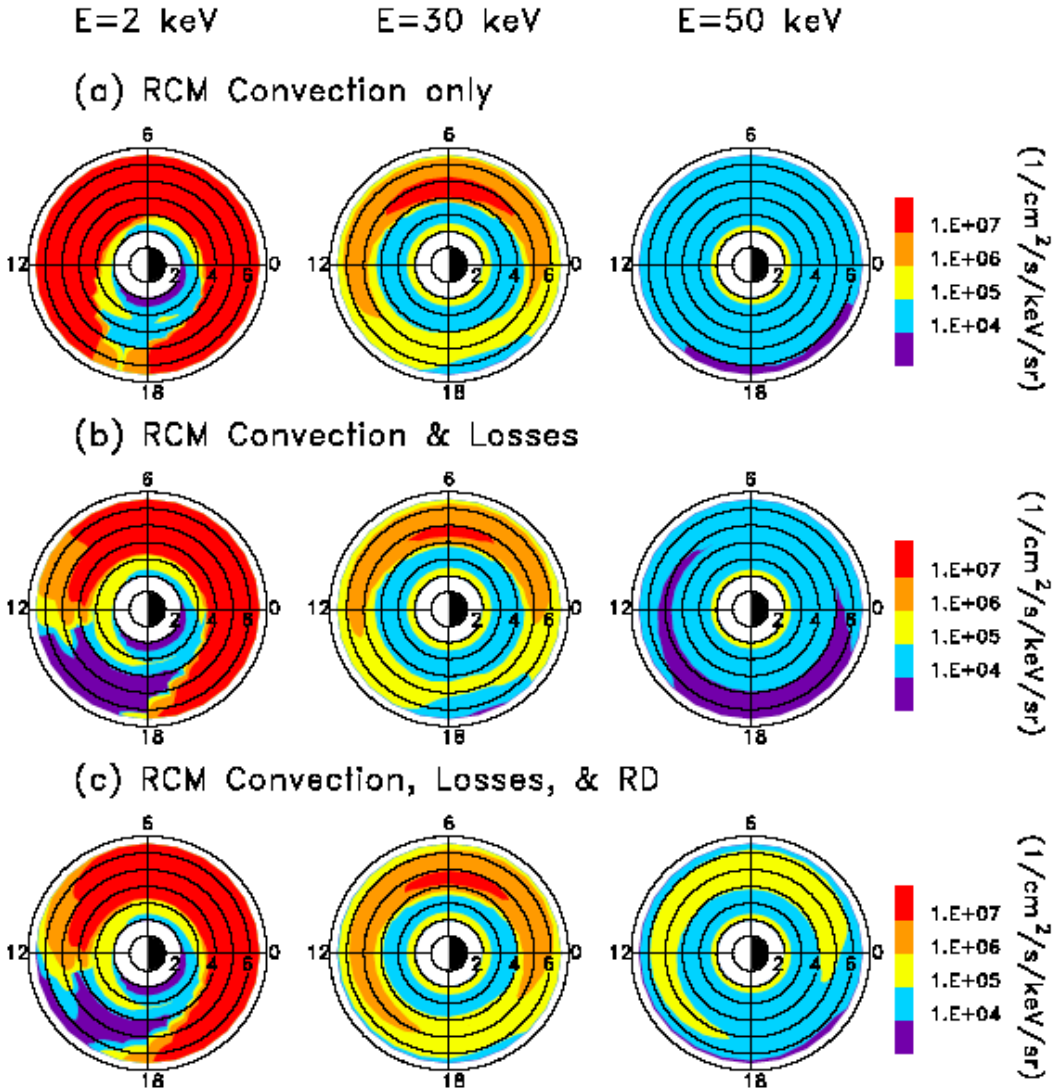

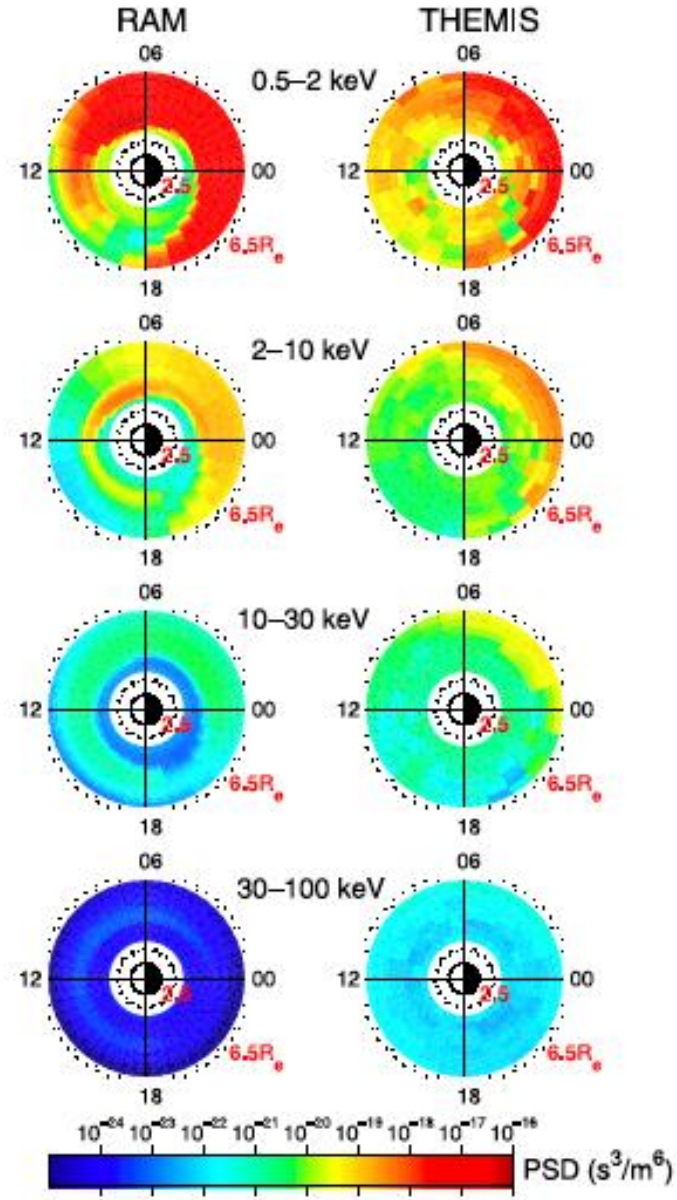

Simulation of Growth of Whistler-mode Chorus

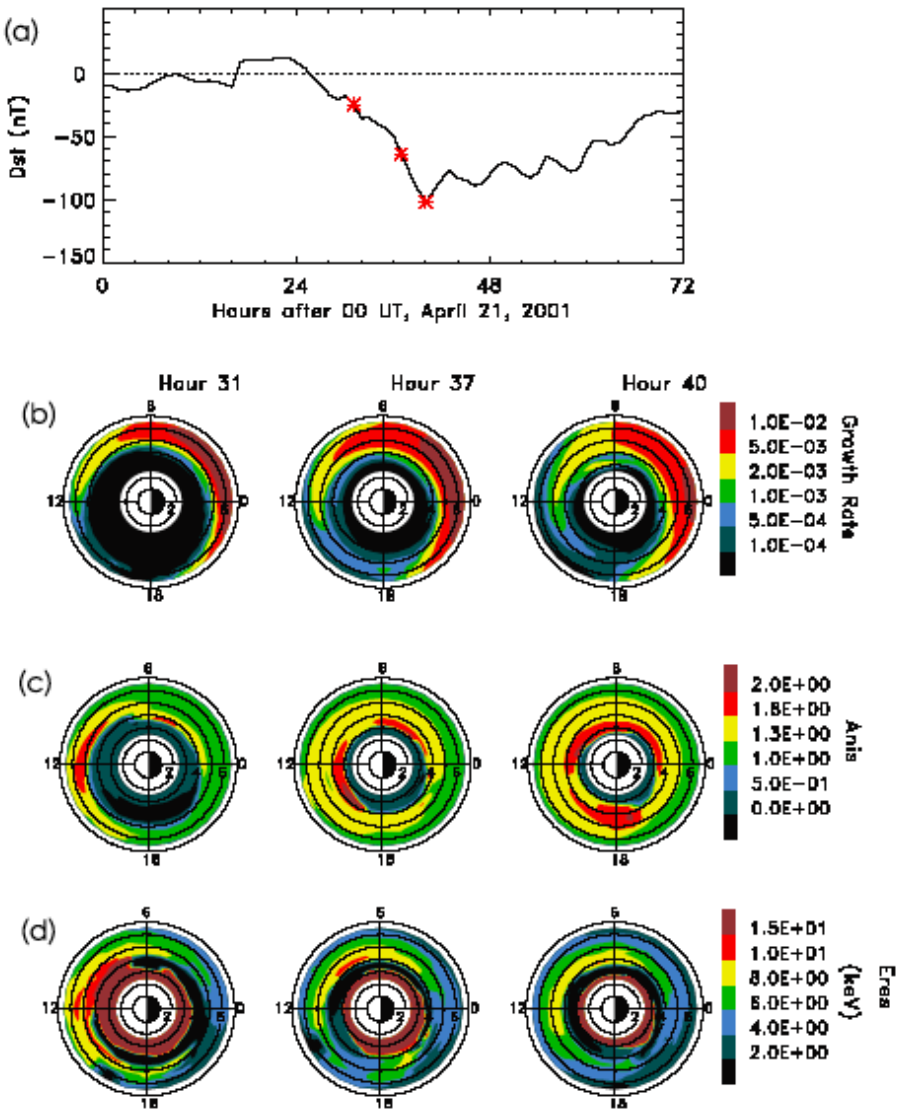

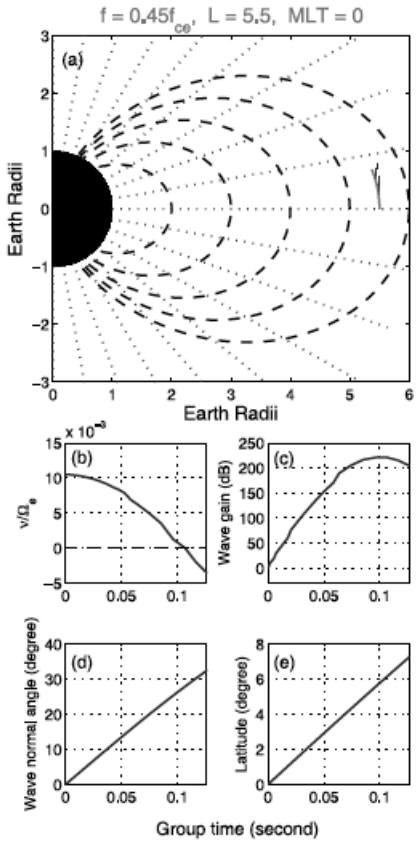

HOTRAY simulations

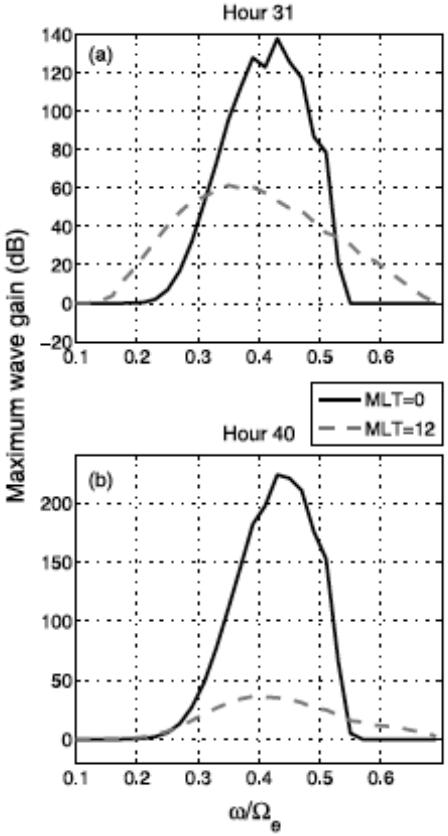

Plasmaspheric Hiss from Chorus

Bortnik, Thorne and Meredith, Nature 2008

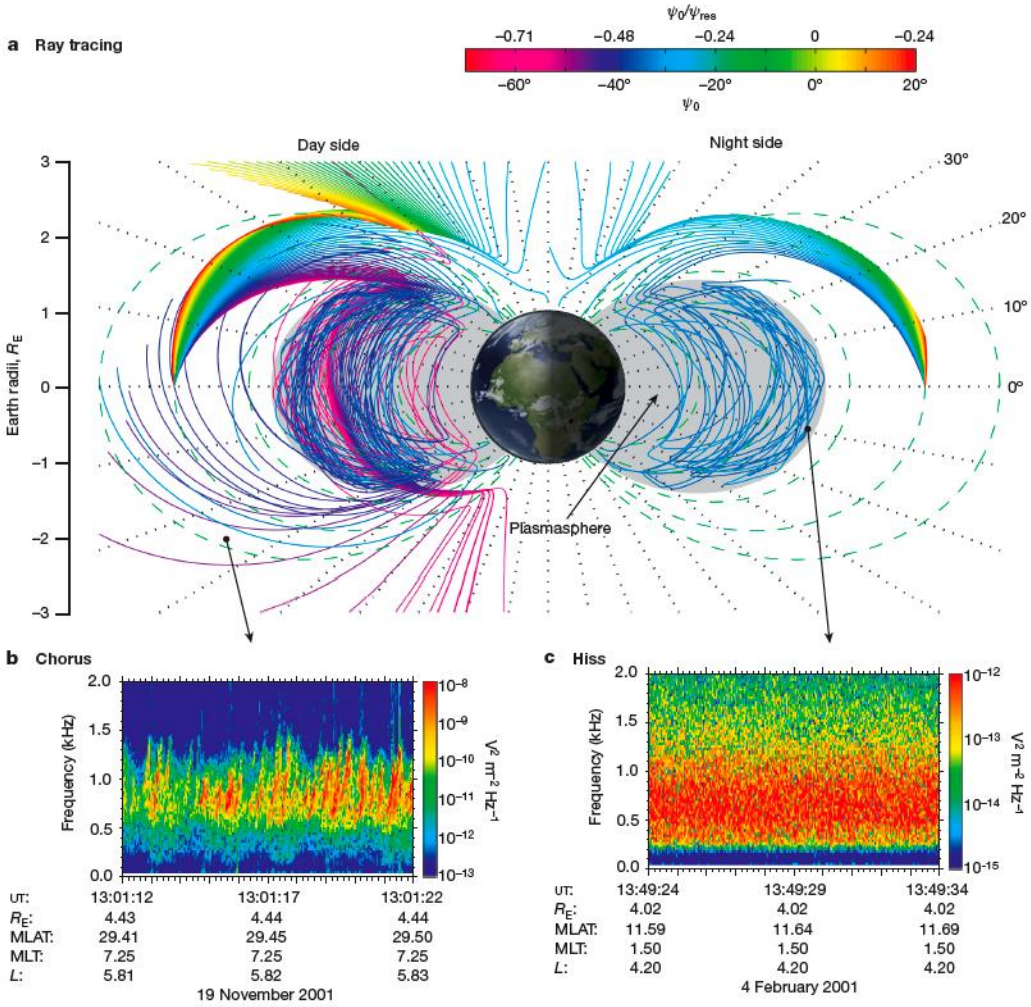

Discrete chorus emissions excited in the outer magnetosphere with wave normals inclined ~ -30° to -50° are able to avoid strong Landau damping, and thus propagate to high latitude, and are there refracted into the plamasphere where they become trapped and eventually merge into incoherent hiss.

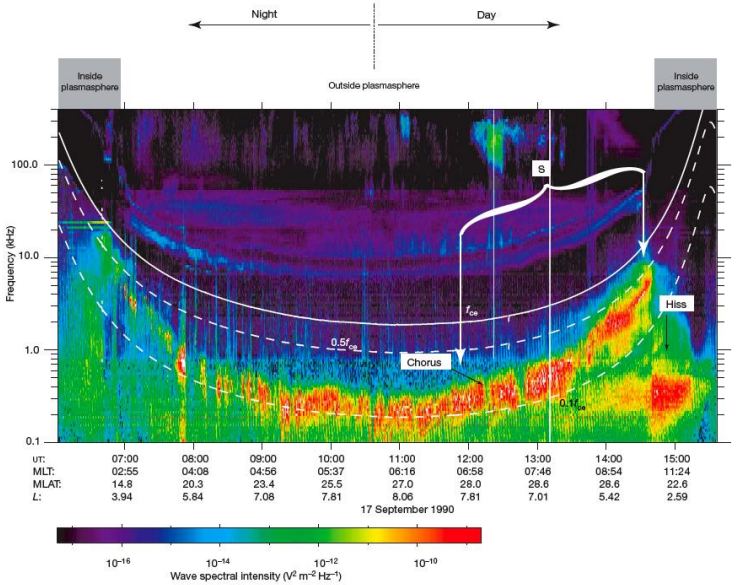

Themis Confirmation of Hiss from Chorus

Bortnik et al. *Science* 2009

QuickTime™ and a
decompressor
are needed to see this picture.

QuickTime™ and a
decompressor
are needed to see this picture.

QuickTime™ and a
decompressor
are needed to see this picture.

QuickTime™ and a
decompressor
are needed to see this picture.

RAM H+ PSD

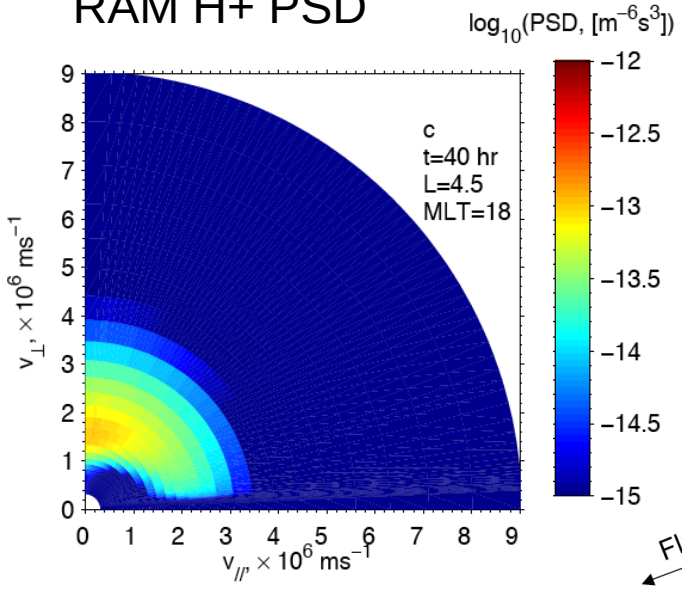

RCM
E-Potential

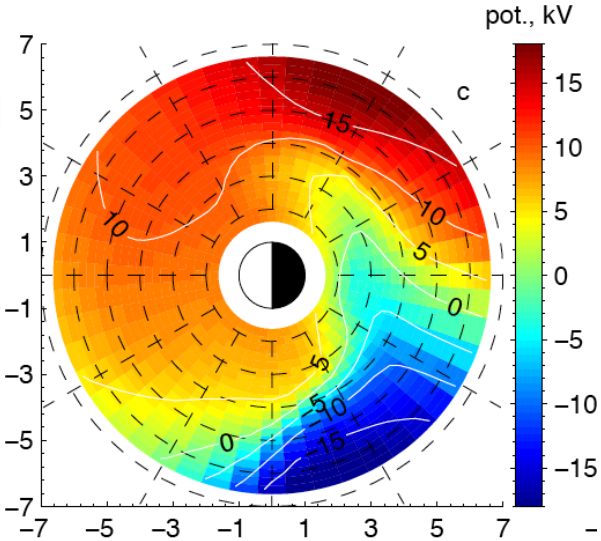

Wave Excitation by Ring Current Ions

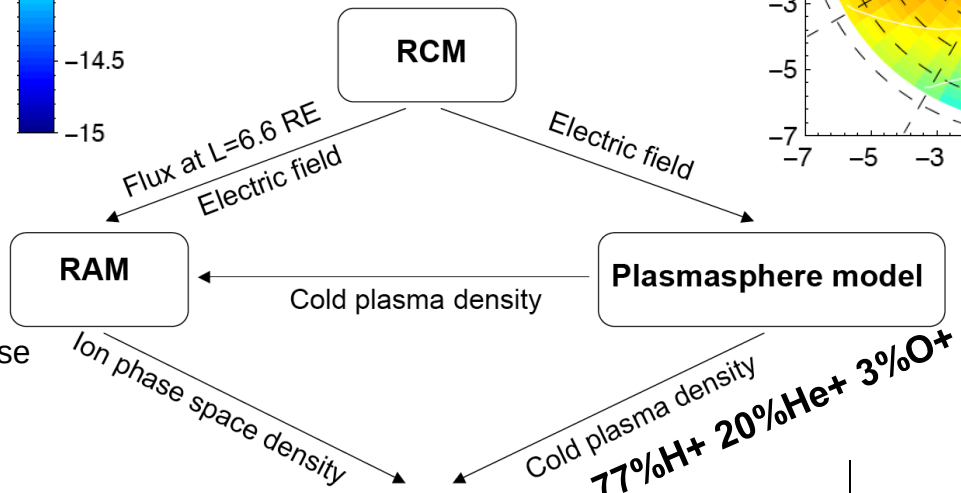

T=40 hr T=48 hr
main phase recovery phase

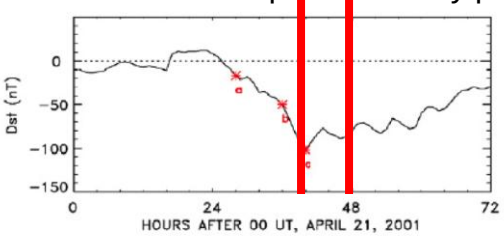

Figure 10: Dst profile for 2001 April 21st storm.

Linear growth rate of EMIC and Magnetosonic waves

Ray Tracing with HOTRAY

Path-integrated gain

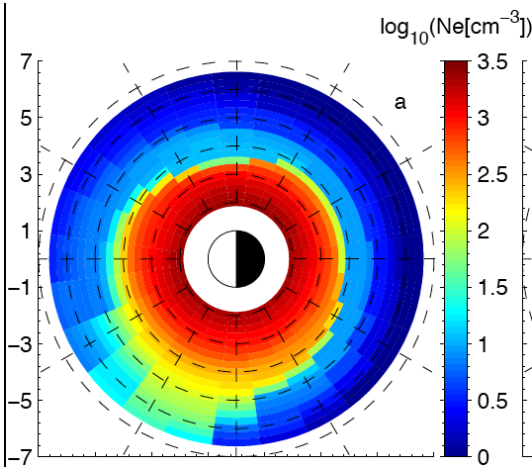

Cold electron density

Chen et al., 2010

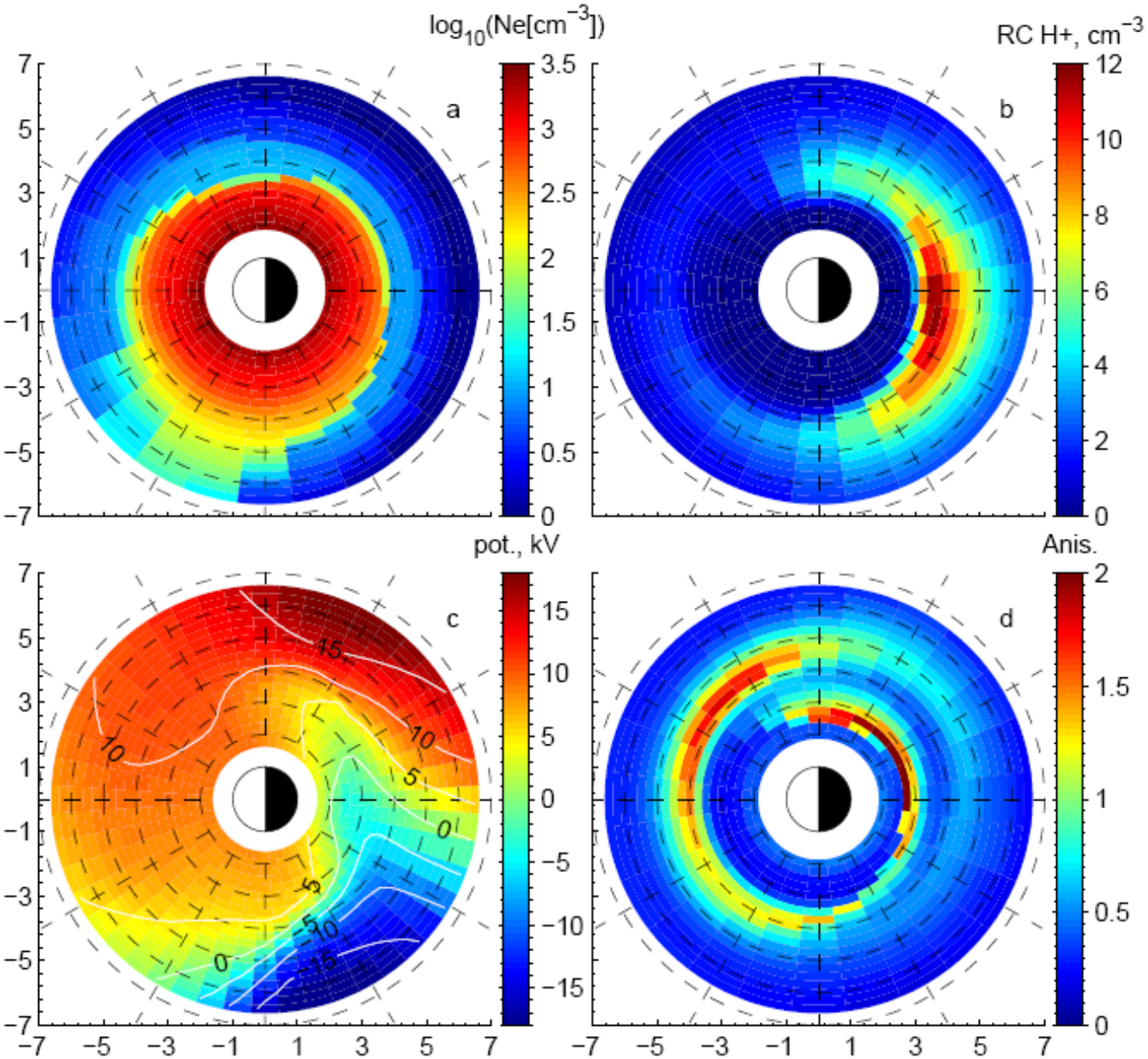

Coupled Simulations During the Main Phase of a Storm

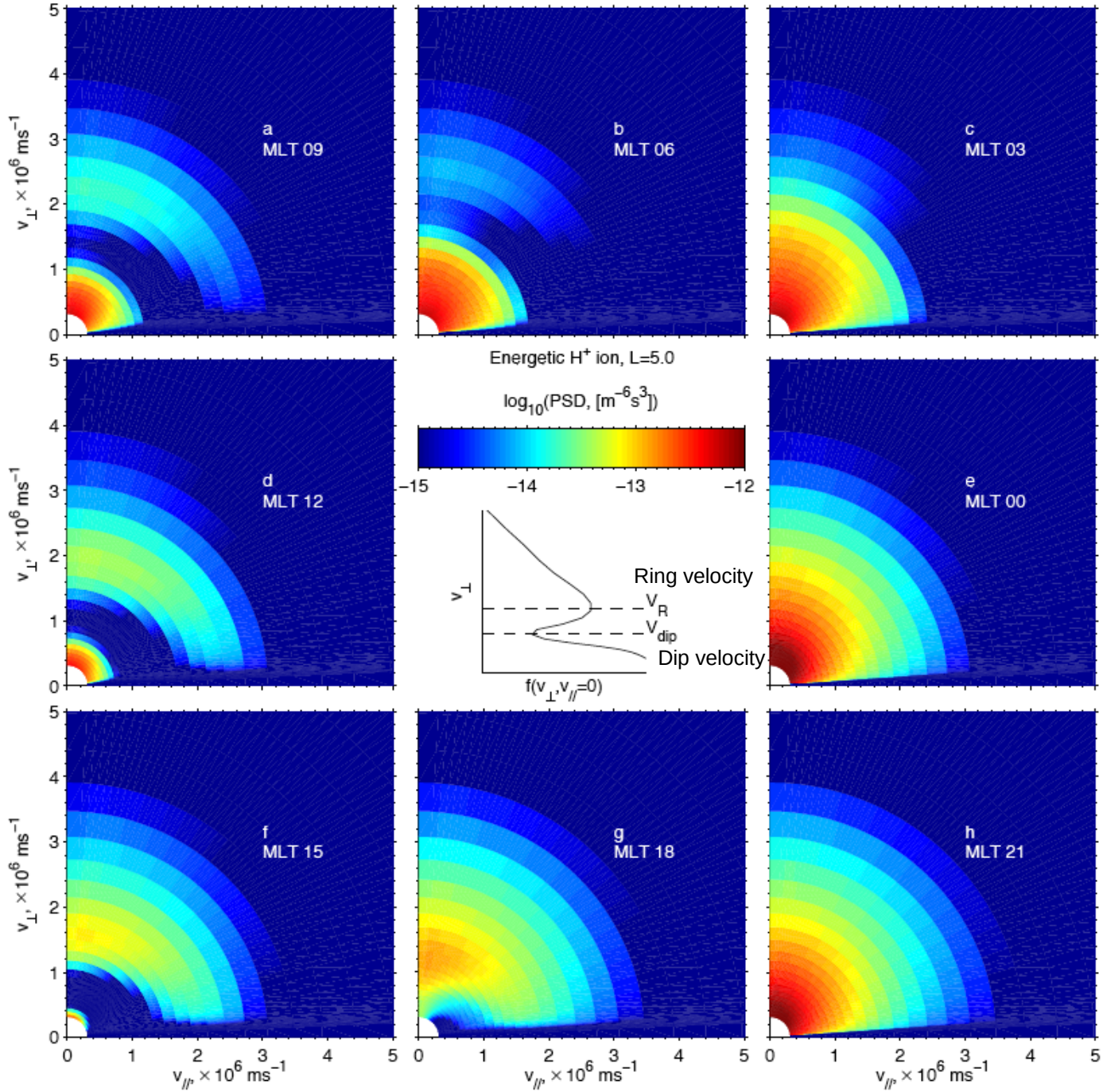

Simulated Energetic H+ Phase Space Density at L=5 During Main Phase

10^6ms-1 -> 5 keV H+

- Bi-Max at night;
- Low energy proton below a few kev extends to noon;
- Higher energy H+ above tens kev drift westward;
- Proton rings (~10-40 kev) develop from morning to dusk;

Proton ring formation is primarily due to energy-dependent drifting

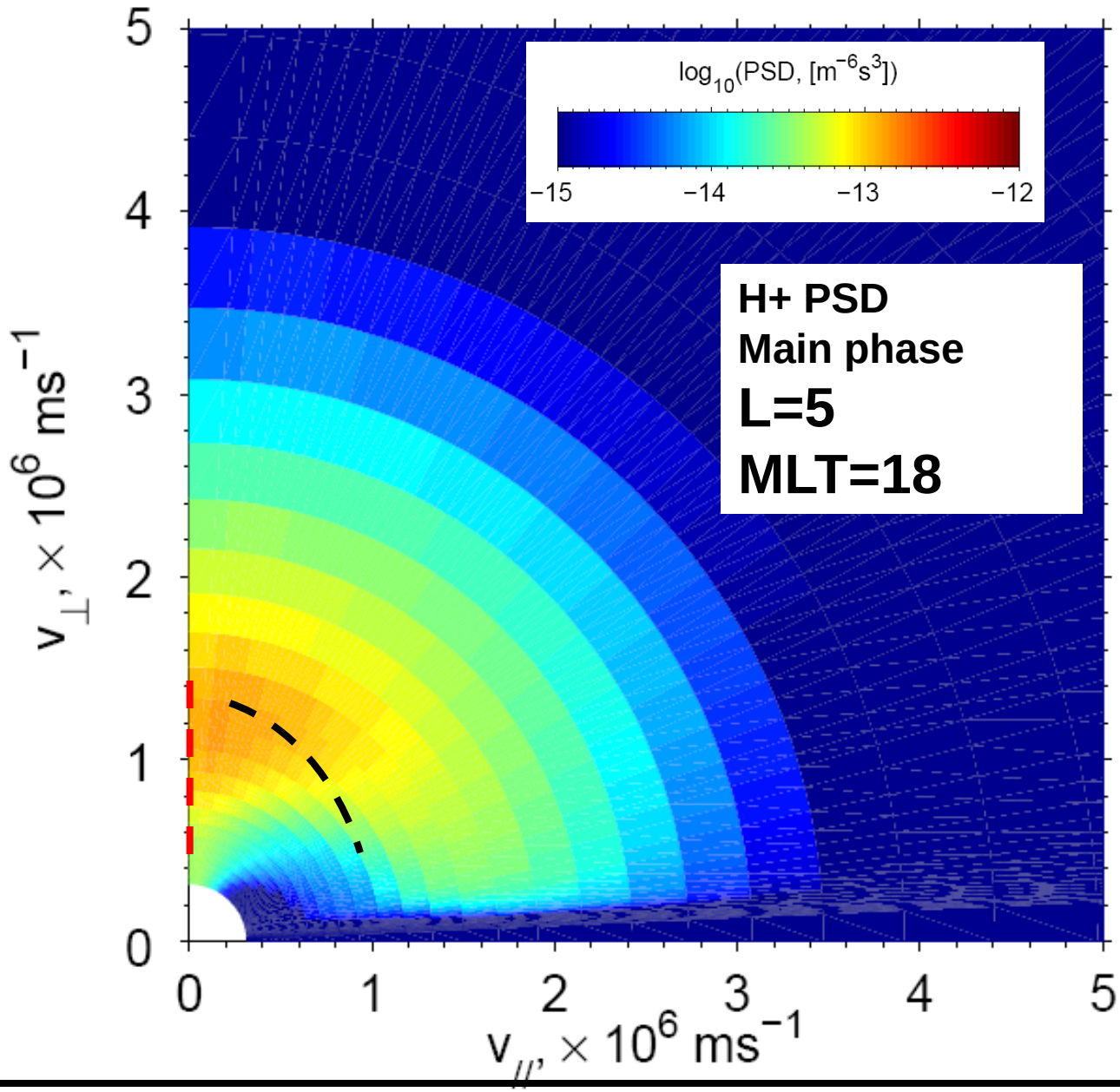

Schematic Diffusion Surface

due to L-mode
field aligned EMIC waves

due to highly oblique
magnetosonic waves

Calculation of local convective growth rate ki
Assumptions 1) Cold plasma dispersion relation
2) small growth rate

$$K_i = \sum_{m=-\infty}^{+\infty} \int_0^{\infty} dv_\perp \left(W_{m,\perp} \frac{\partial f}{\partial v_\perp} + W_{m,\parallel} \frac{\partial f}{\partial v_\parallel}\right)\Big|_{v_\parallel = v_{res\parallel}}$$

[Kennel 1966, Chen et al., 2010]

Path Integrated Gain and Spectral Properties of Excited EMIC Waves

Chen et al., 20010

Hour 48, storm recovery

Strongest wave gain confined to the edge of the plume and nightside plasmapause

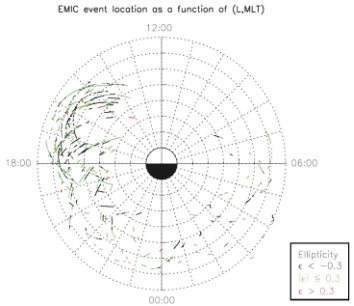

Electron minimum resonant energies with waves having more than 30 db gain near the equator.

QuickTime™ and a
decompressor
are needed to see this picture.

QuickTime™ and a
decompressor
are needed to see this picture.

Minimum electron cyclotron resonant energy with excited EMIC waves in the equatorial region (Gain >30 dB)

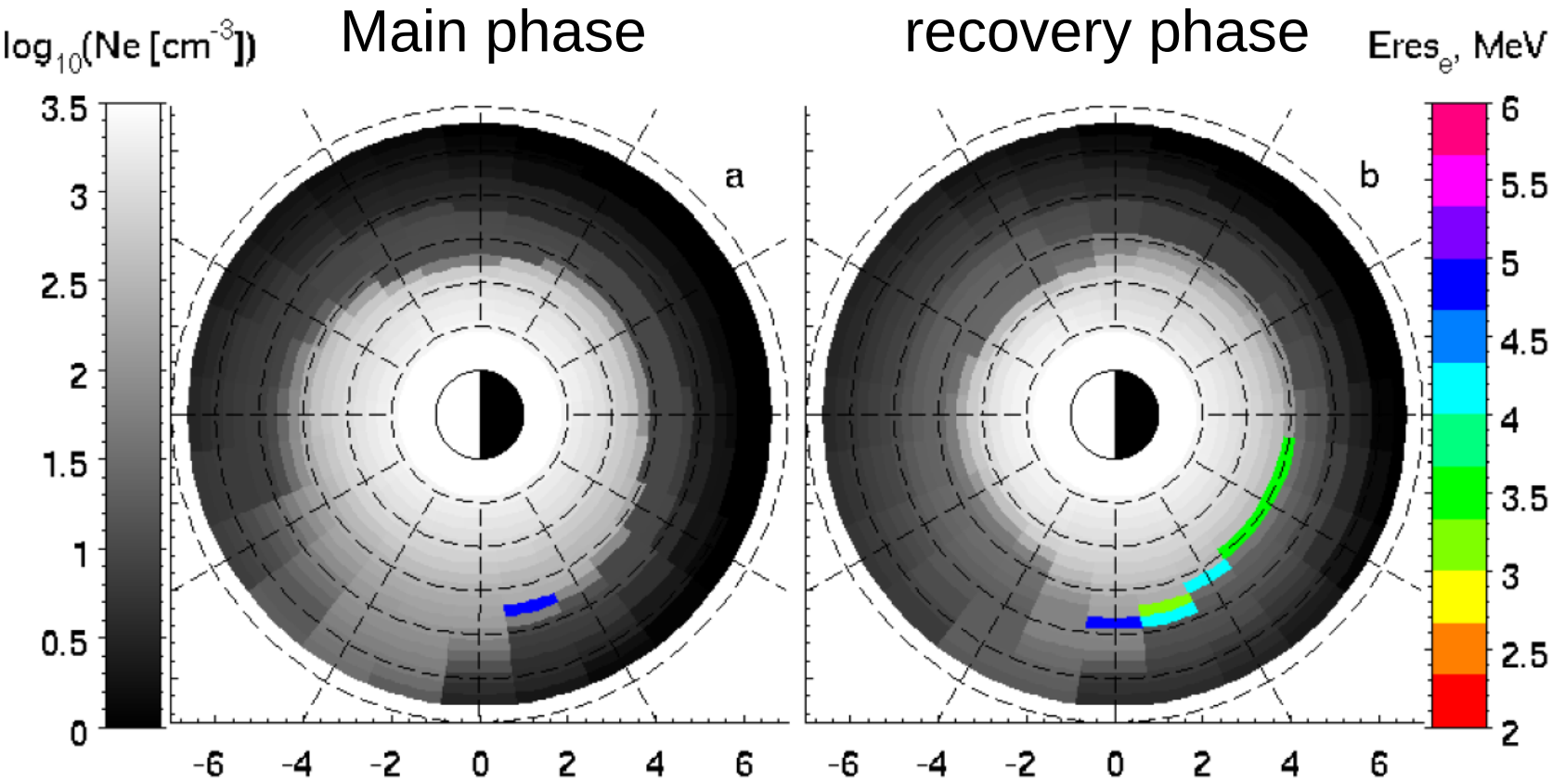

~ 5 MeV during main phase; > 3 MeV at recovery phase

But no fine scale density fluctuation is included.

EMIC Excitation and Electron Scattering in Structured Plumes

Chen et al., 2009

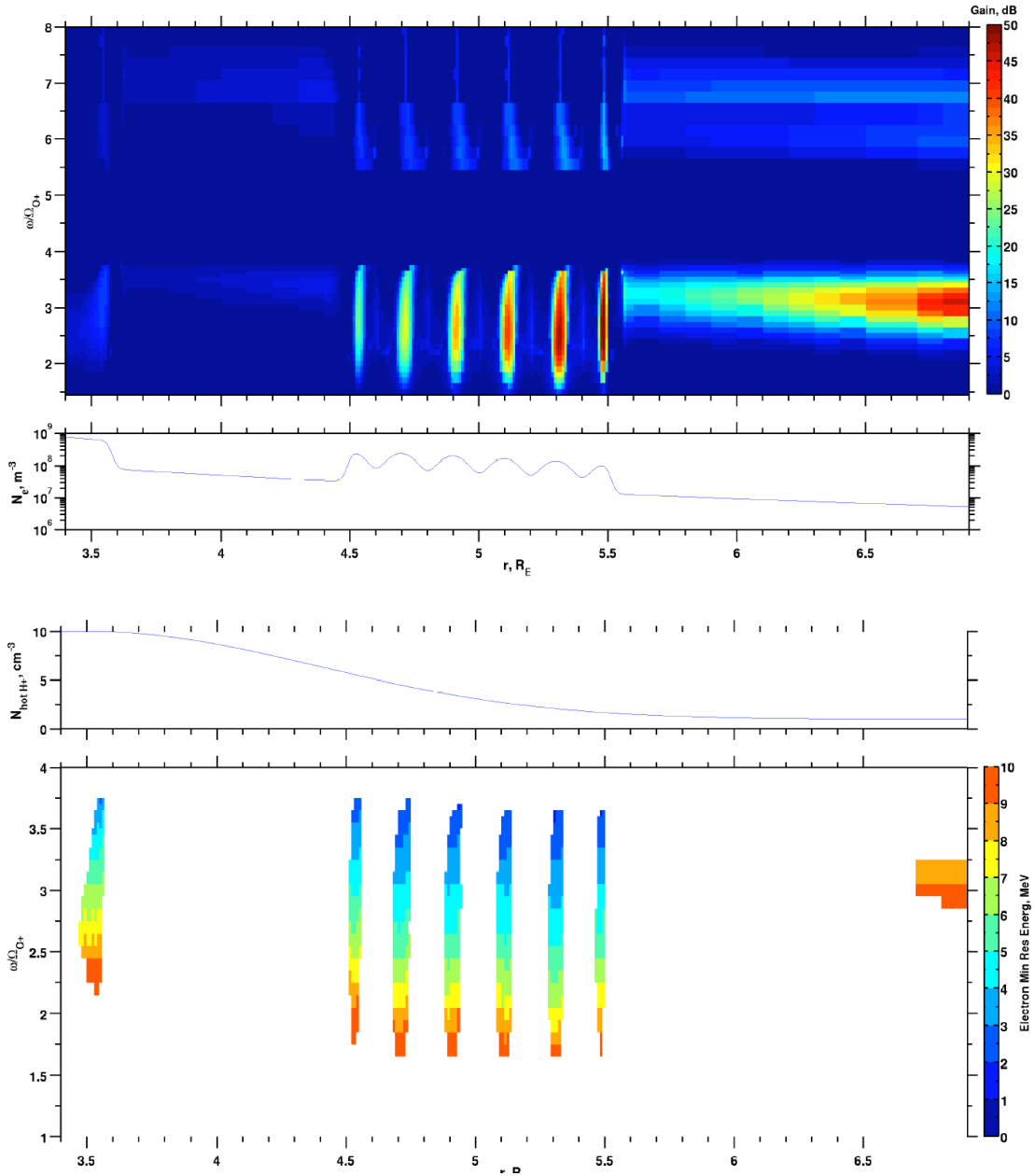

EMIC waves below the Helium gyrofrequency are preferentially excited in plumes with radial density structure.

A bi-Maxwellian ring current ion distribution with N-1, Tperp=50 keV and Tpar = 25 keV is used.

Electron resonant energies with waves experiencing more than 40 db gain are typically more than 2 MeV in plumes and near the plasmapause, but > 8 MeV in the trough.

Schematic illustration of magnetosonic wave instability

Maximum instability occurs at frequencies where the peak in W_{perp} lies in positive df_{perp}/dv_{perp} range.

As V_A increases or V_R decreases, unstable waves move to higher frequency.

$$K_i \sim \int_o^\infty dv_\perp W_\perp \frac{\partial f}{\partial v_\perp}\Big|_{v_{||}=0}$$

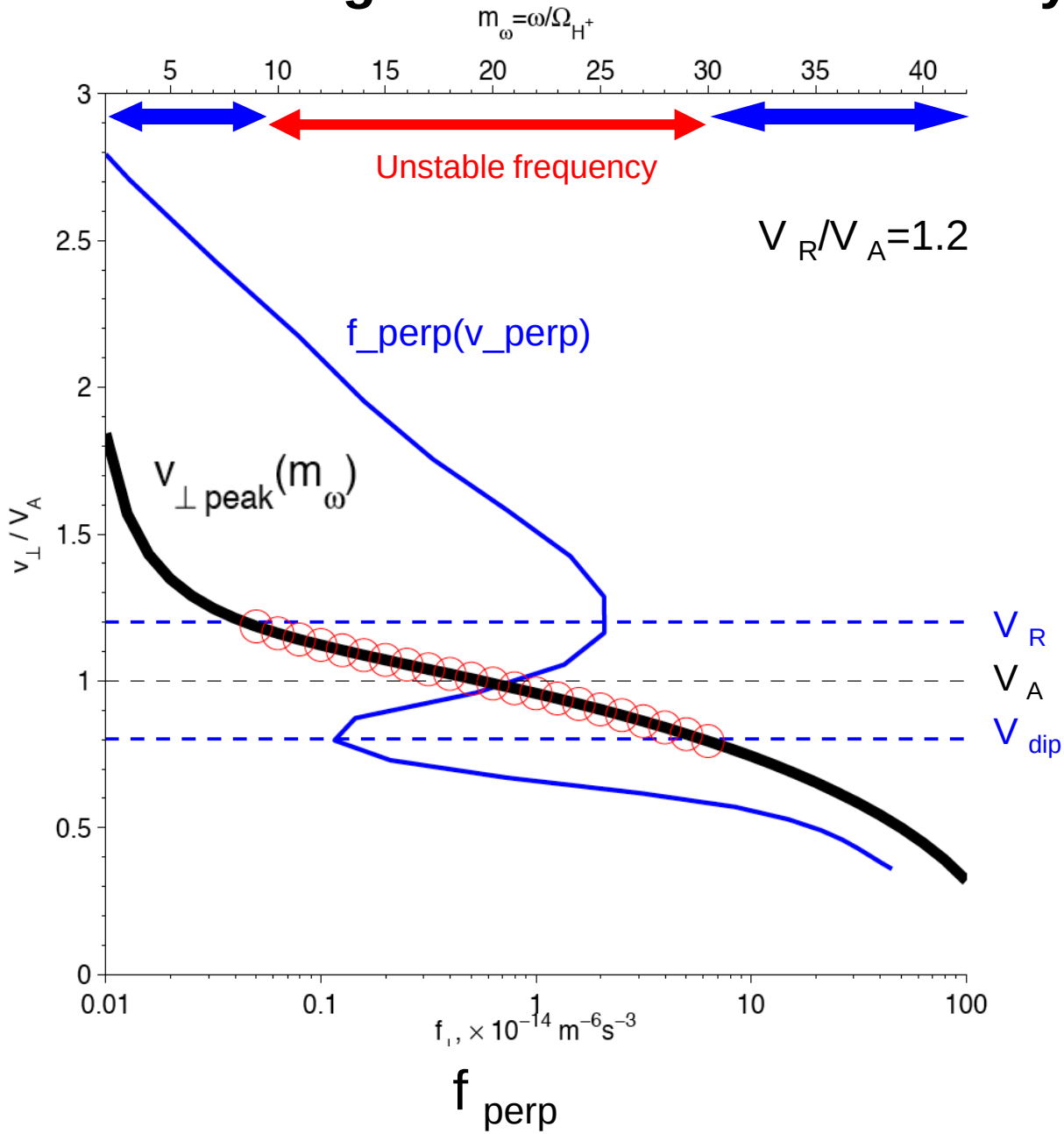

Proton Ring Characteristics During Storm

PSD peak along vp

plasmapause

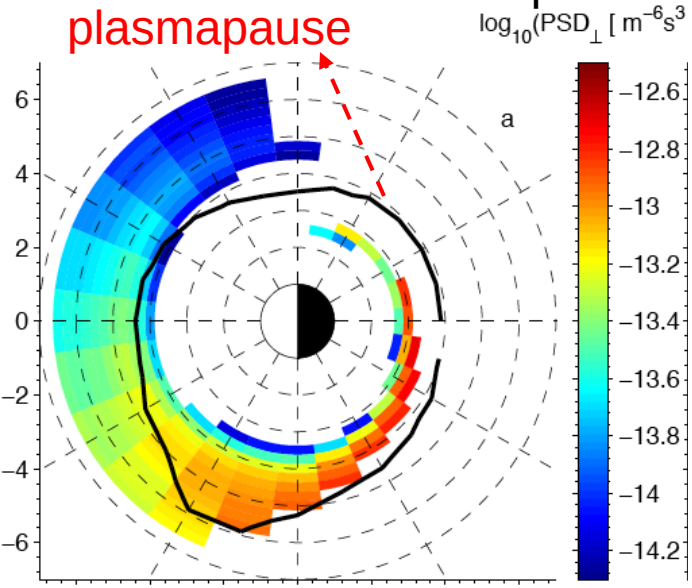

Proton rings occur over a broad spatial region:

1) Deep inside plasmasphere at night;
2) Inside the plume on the duskside;
3) In the trough on the dayside.

Ring energy a few to tens kev
Dip energy a few to 10 kev
Both decrease at larger L and earlier MLT

Ring energy $E_R = \frac{1}{2} m_p V_R^2$

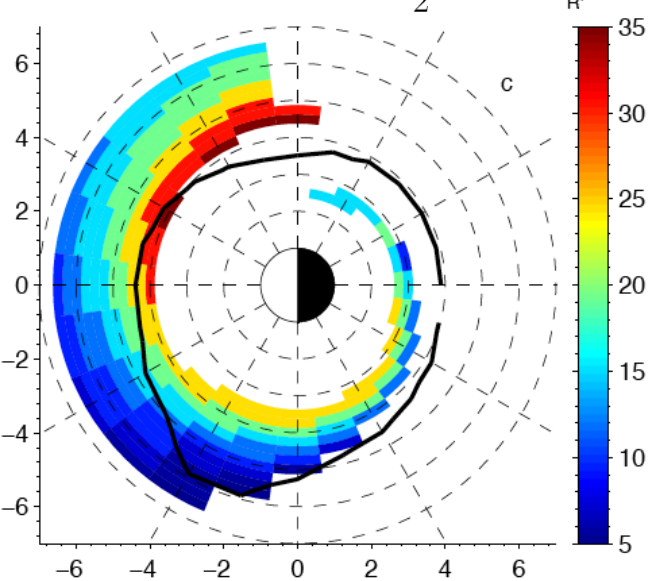

Dip energy $E_{\mathrm{dip}} = \frac{1}{2} m_p V_{\mathrm{dip}}^2$

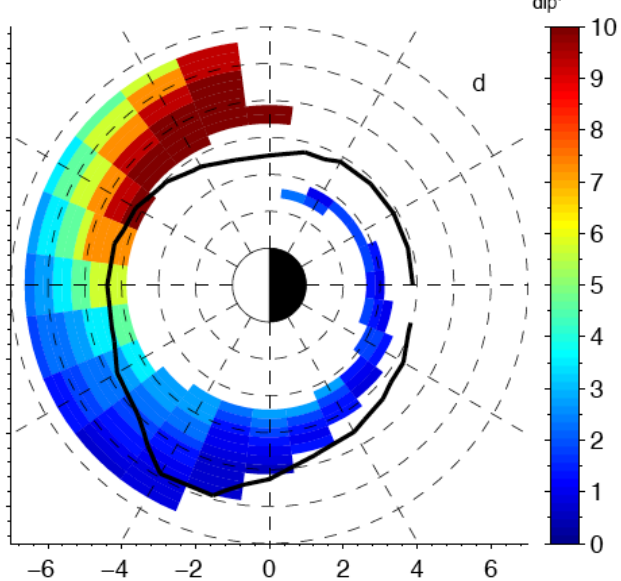

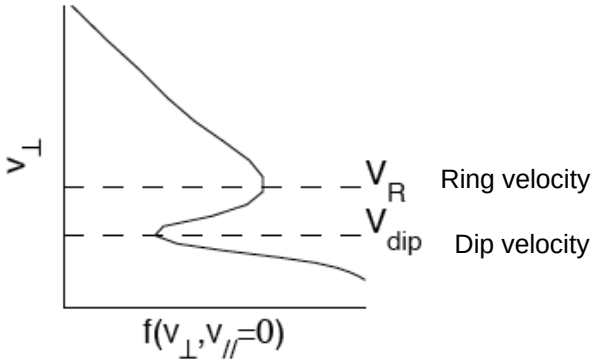

MS Convective Growth Rate K_i (freq, MLT, L

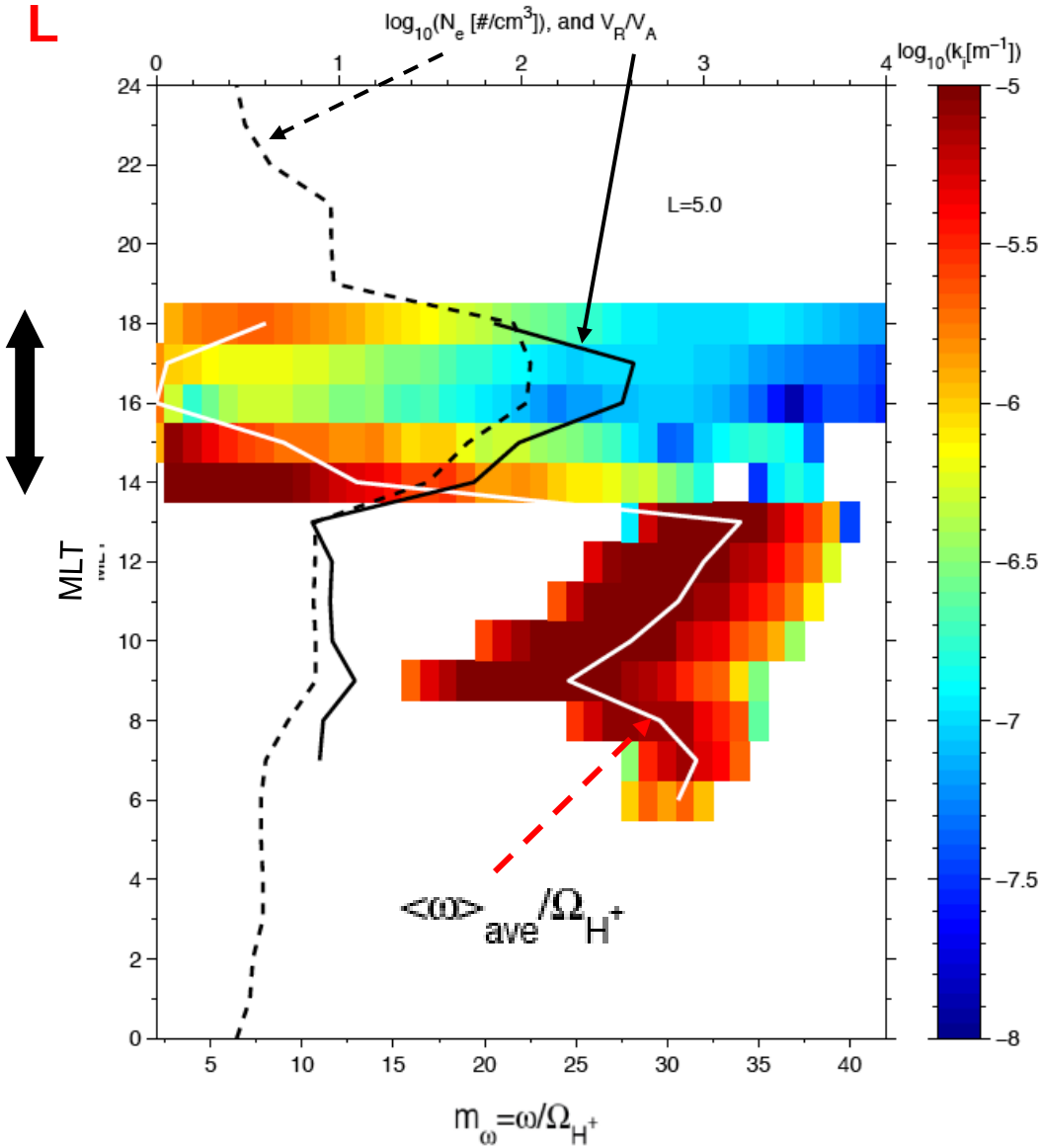

Ne (MLT)

V_R/V_A (MLT)

White solid shoes center of unstable frequency band

- In the trough from dawn to post-noon, instability occurs at relatively high harmonics of the proton gyrofrequency.
- Inside the plume, instability occurs over a broad range of wave frequencies, with peak at low harmonic proton gyrofrequencies.
- The center of frequency spectrum is modulated by the ratio V_R/V_A. As the ratio increases, instability tends to occur at lower frequency.

Chen et al. 2010

The Center Frequency of Unstable Magnetosonic Waves

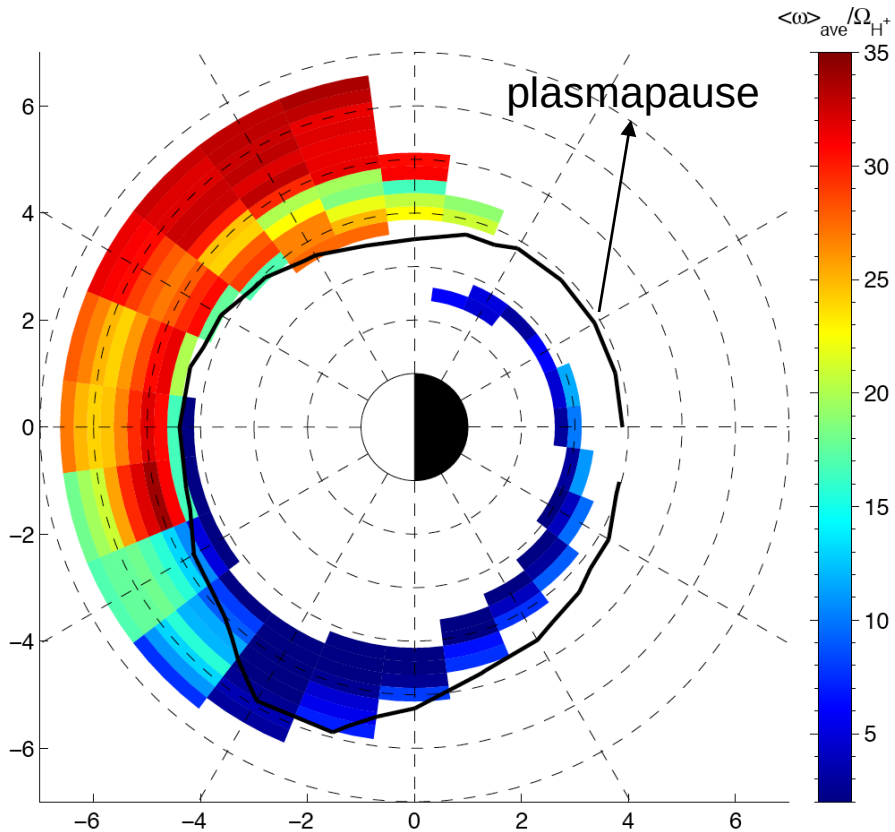

➢MS waves at low frequencies (< 10 proton gyrofrequency) tend to be unstable in the high density region.

➢MS waves at relatively high frequencies (> 20 proton gyro frequency) are unstable outside the plasmasphere on dayside.

Note that this pattern is obtained based on local growth rate calculation. No propagation effect is taken into account.

Electron Scattering by Equatorial Magnetosonic Waves

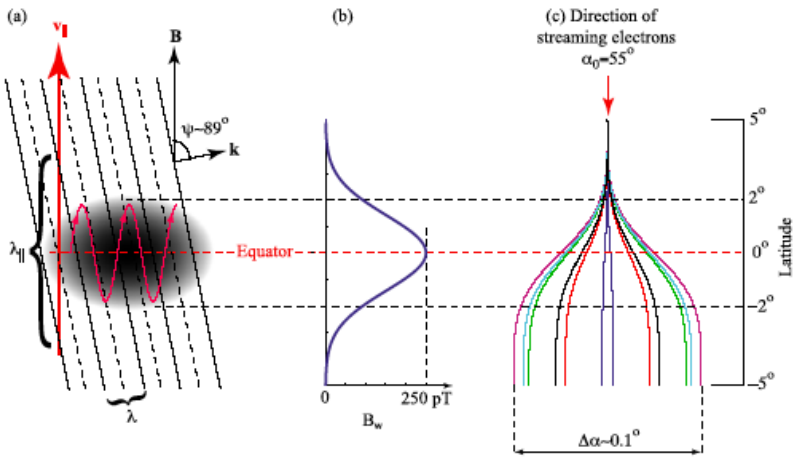

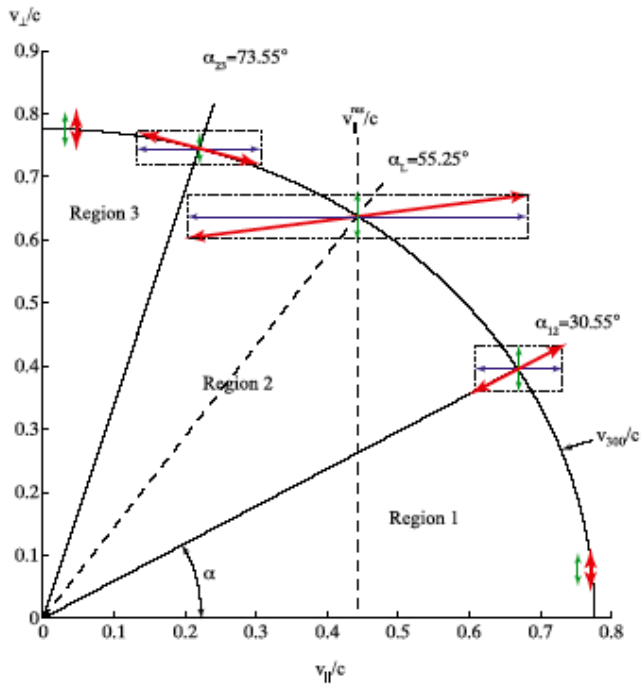

Bortnik and Thorne, 2010

Evidence for both Landau resonant acceleration and non resonant transit time scattering

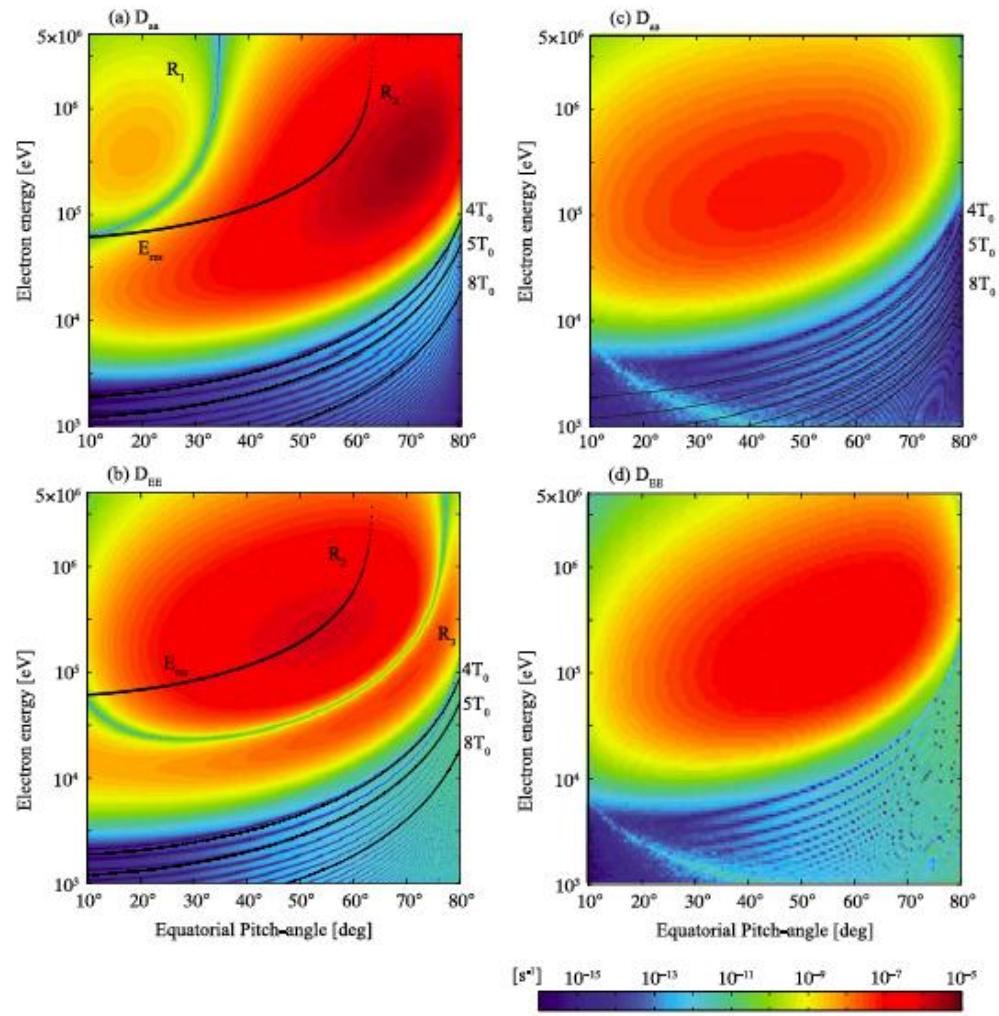

Origin of Earth's Diffuse Aurora

Thorne et al., 2010

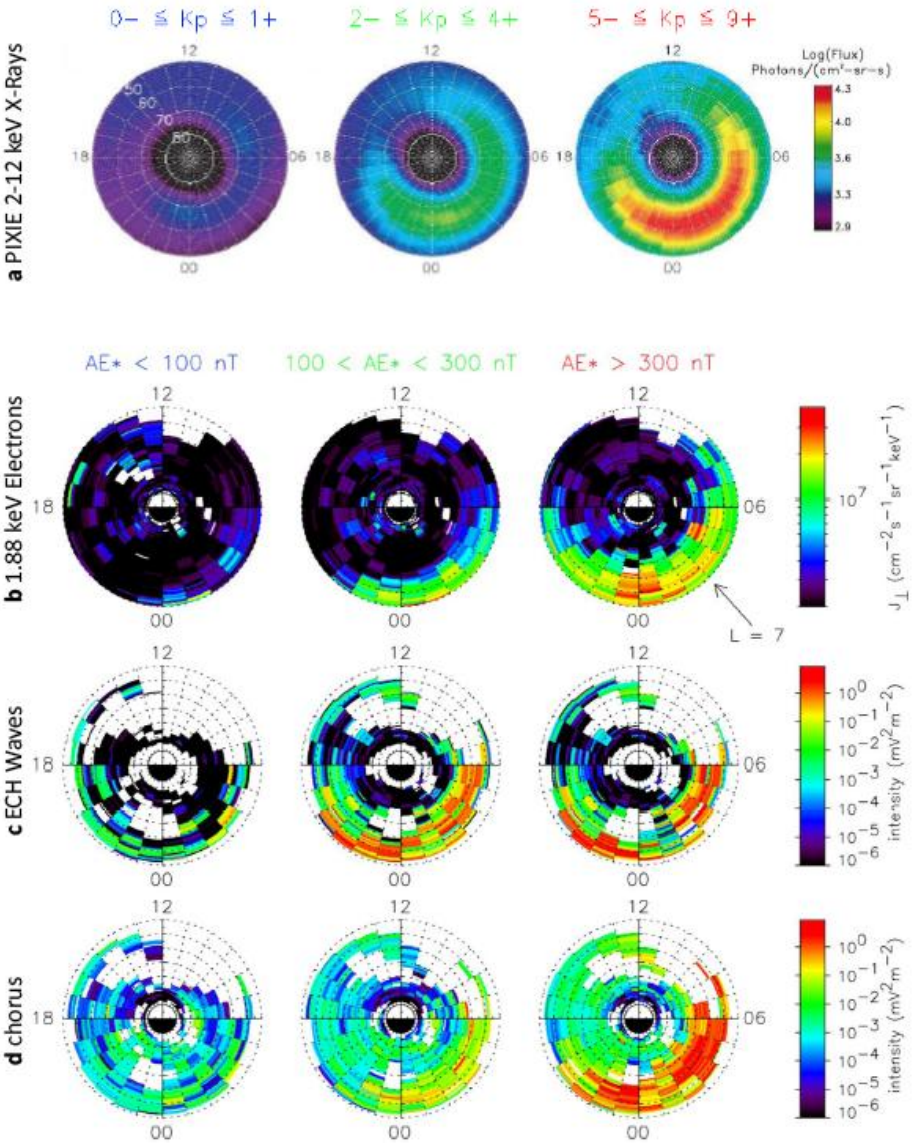

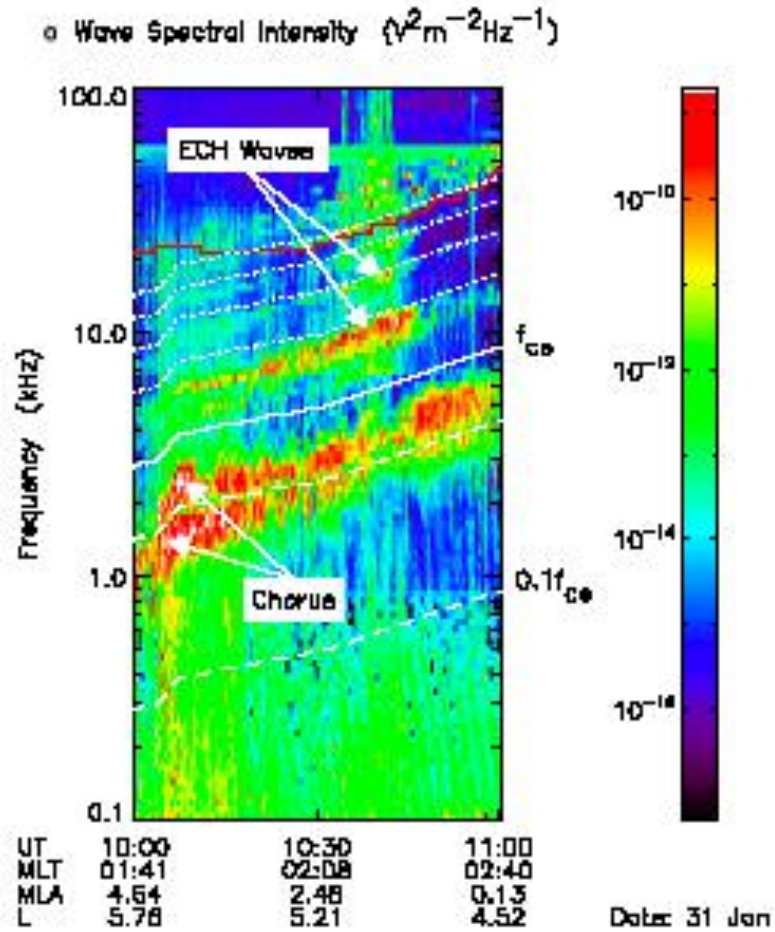

CRRES Analysis of Power in Different Harmonic Bands: Used for the Evaluation of Diffuse Auroral Scattering Rates

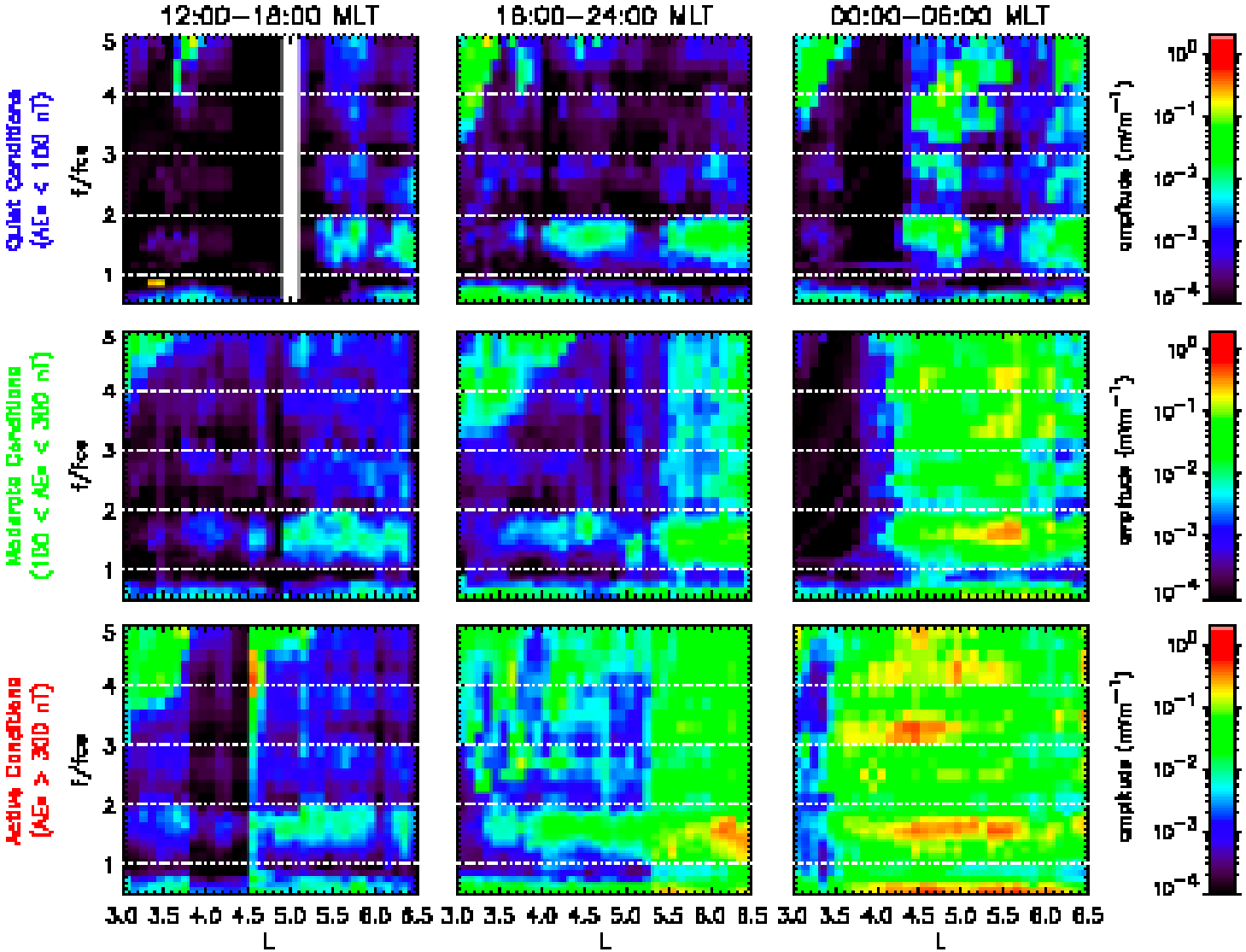

Nightside Scattering Rates at L=5 and Resultant PSD Evolution

Diffusion Rates

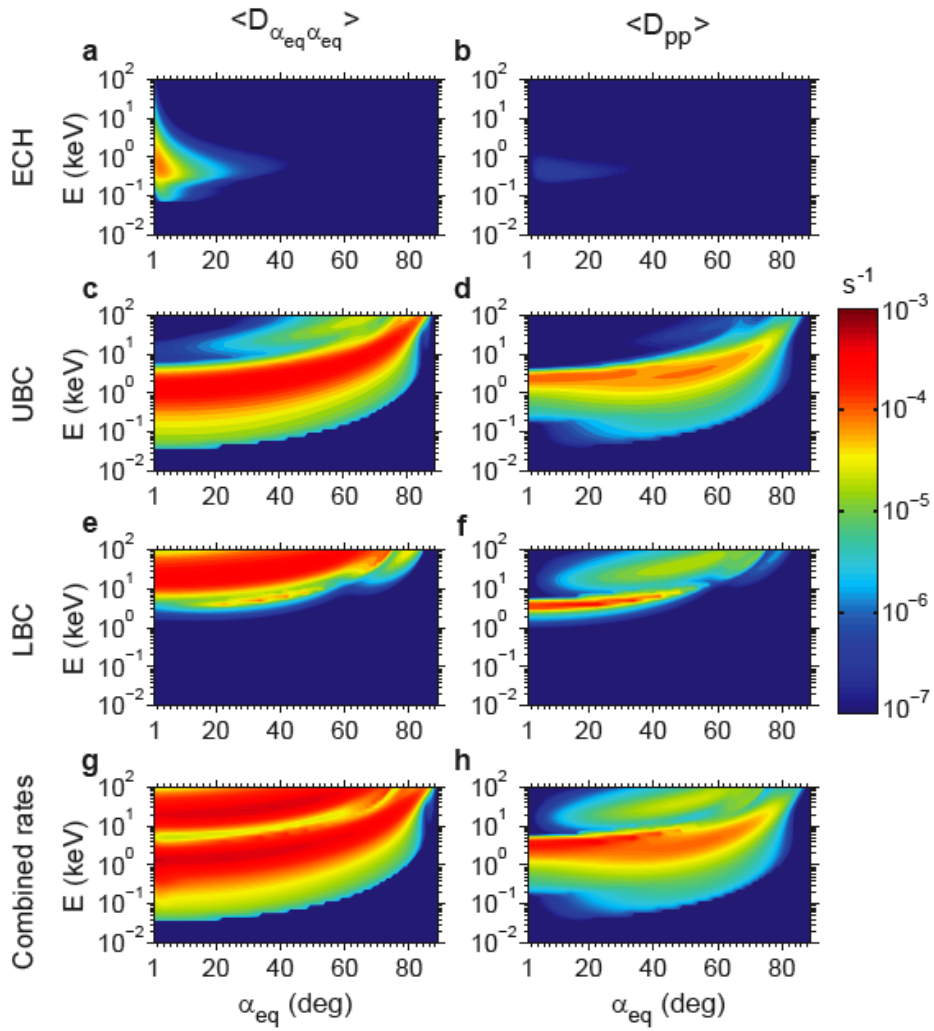

CRRES observations

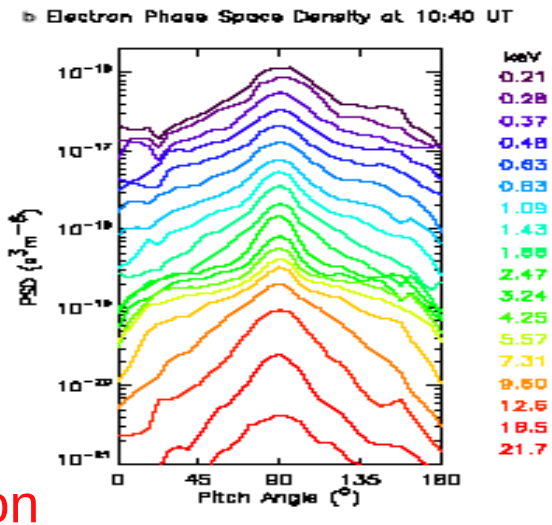

PSD evolution

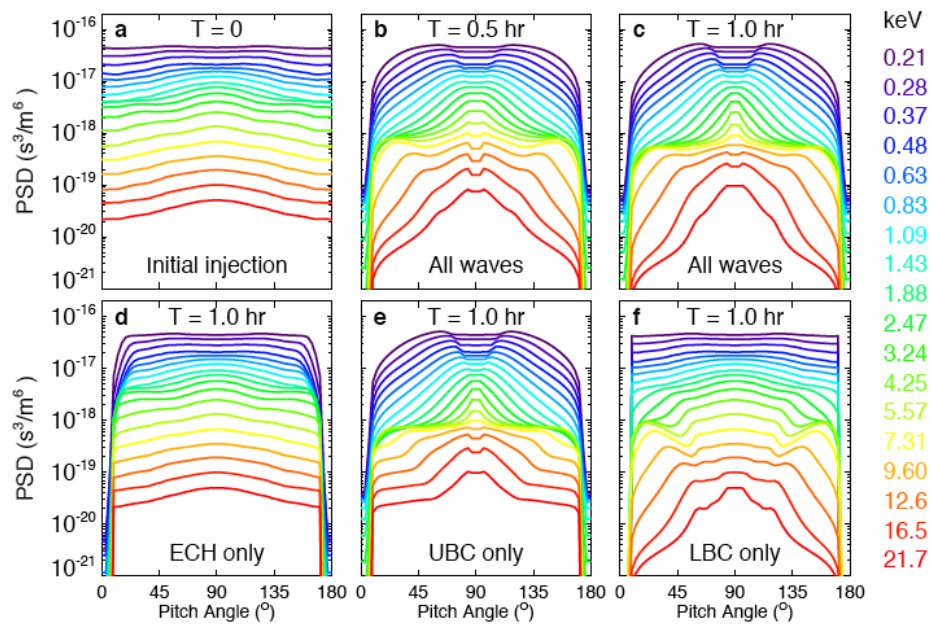

Major Remaining Challenges

1) Better observations of P(ω, k, L, λ, MLT)

   EMIC: Improved observations of P(ω, k, L, λ, MLT), especially near the He gyro.

   Magnetosonic: better statistics on global distribution, information on fine structure, and identification of source region

   Chorus: Better information on anglular distribution from observations and 3D ray tracing, modulation of instability.

   Hiss: Confirmation of origin from chorus, use of 3D ray tracing to obtain angular distribution throughout the plamasphere

   ECH: Poor CRRES coverage on dayside, data mining from SCATHA THEMIS and other satellites

   ULF: Does MHD provide realistic global distribution of waves since substorm physics is missing

2) Inclusion of non-linear scattering into transport codes

   Possible advective transport: more efficient temporal changes

3) Self consistent 4D Modeling

   Global excitation of waves based on modeled f(α,E,L,MLT,t), inclusion of feedback of wave scattering on injected particles (e.g.,UCLA coupled RCM/RAM/HOTRAY)

Modeling Preparations for RBSP launch in 2012

1) Data mining of P(ω, k, L, λ, MLT) for relevant VLF/ELF plasma waves
2) Development of better time-dependant models of the plasmapause and plume
3) Better modeling of the global distribution of ULF waves and associated D_{LL}
4) Continued development of 3D and 4D Transport Codes: f(α,E,L,MLT,t)
5) Development of data assimilation codes to place the spatially and temporally limited RBSP data into a global context